

Imaging of shoulder arthropathies

Maria Douka¹, Evangelia E. Vassalou², Athena P. Plagou³, Apostolos H. Karantanas^{4,5}

¹Department of Radiology, Athens Naval Hospital, Athens, Greece

²Department of Medical Imaging, General Hospital of Sitia, Greece

³Ultrasound Unit, Private Radiological Institution, Athens, Greece

⁴Departments of Radiology, Medical School - University of Crete and Medical Imaging, University Hospital, Heraklion, Greece

⁵Advanced Hybrid Imaging Systems, Institute of Computer Science, Foundation for Research and Technology (FORTH), Heraklion, Greece

SUBMISSION: 7/5/2020 - ACCEPTANCE: 27/8/2020

ABSTRACT

The glenohumeral joint is a complex anatomical structure characterised by hypermobility and large synovial and articular surfaces. Shoulder pain is a common clinical complaint in adults, related to a wide spectrum of disorders, including synovial disorders such as inflammatory and crystal-induced arthropathies, rotator cuff disease and osteonecrosis. Primary degenerative osteoarthritis is rarely seen because the glenohumeral joint is non-weight-bearing. In the presence of advanced osteoarthritis of the glenohumeral joint in

patients without previous trauma or infection, radiologists should explore other underlying causes such as crystal-induced arthropathy and Charcot's neuropathic arthropathy. Young adults may show early-onset osteoarthritis as a complication of previous trauma and long-standing synovial osteochondromatosis. This pictorial review presents the pathophysiology, important clinical aspects and the main imaging findings which allow an accurate diagnosis of glenohumeral joint arthritis.



KEY WORDS

Shoulder Joint/diagnostic imaging; Shoulder Joint/pathology; Magnetic Resonance Imaging; Joint Diseases/diagnosis; Radiography; Osteoarthritis/diagnostic imaging



CORRESPONDING AUTHOR, GUARANTOR

Apostolos H. Karantanas, Medical School, University of Crete, Voutes, Heraklion 71110, Greece, Email: akarantanas@gmail.com

Introduction

Shoulder pain is one of the commonest symptoms affecting the general population, with a prevalence of up to 30% [1]. Pain-generating sources are both the glenohumeral (GHj) and acromioclavicular (ACj) joints, as well as the rotator cuff (RC) and the capsuloligamentous structures [2]. Although radiologists maintain a high index of suspicion regarding RC disease and labral pathology, arthropathies are often overlooked, especially in the context of limited or lacking specific clinical information.

A wide spectrum of differential diagnoses is described under the umbrella of shoulder arthropathy (Table 1) [3]. Although history and clinical examination have a vital role in the diagnostic algorithm, imaging is a crucial part of the diagnostic approach. Patients with GHj or ACj arthritis usually present with a gradually worsening pain. The ACj arthritis has typically localised pain which is exacerbated upon pressure over the joint. GHj arthritis on the other hand has a vague pain location, which typically worsens on active and passive motion [1].

In shoulder arthritis, plain radiographs (PR) are the imaging modality of first choice. A standard anteroposterior (external rotation of the hand) view allows visualisation of the AC joint. The “Grashey” or posterior oblique anteroposterior view assesses the GHj. When PR are inconclusive, MRI, due to its superb contrast resolution, allows for synchronous assessment of the osseous, cartilaginous and soft-tissue structures of the joint [4]. Despite the high prevalence of GHj arthritis, there is scarce literature regarding the systemic description of the entities related to this condition [5, 6]. In this pictorial essay, we focus on arthropathies affecting the GHj which is a commonly underestimated topic among radiologists. Important pathophysiological and clinical aspects as well as key imaging findings, with emphasis on MRI, will be presented in an attempt to increase the awareness of radiologists for early diagnosis and proper patient management.

1. Inflammatory arthritis

Imaging modalities such as PR, MRI and ultrasound (US) have an integral role in diagnosing and monitoring of inflammatory disorders of the GHj, including rheumatoid arthritis (RA) and seronegative spondylarthropathies (SpA) [7].

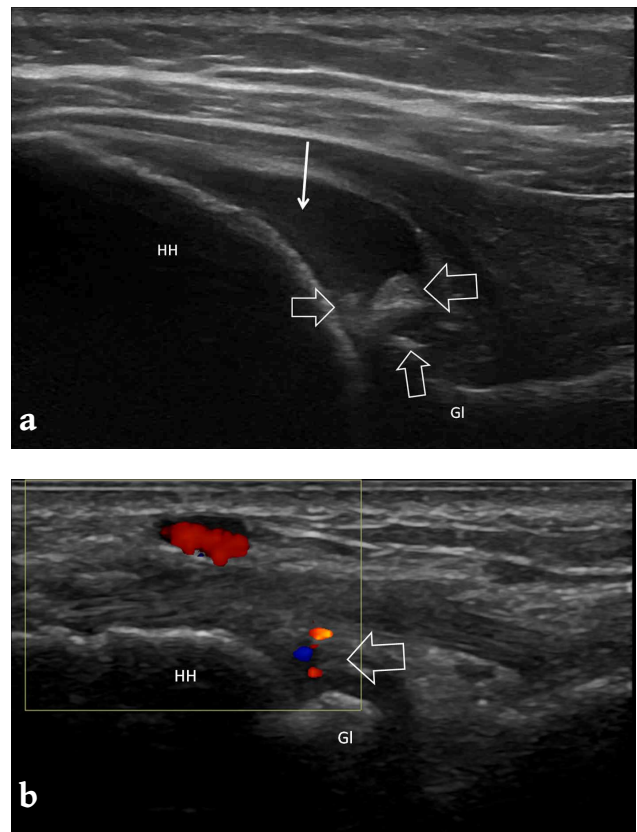


Fig. 1. Ultrasonography in rheumatoid arthritis. **a)** Posterior approach showing the glenohumeral joint effusion (thin arrow) and the synovitis with the presence of “rice bodies” (open arrows). **b)** Posterior approach in another patient showing synovitis with positive Doppler signal (arrow). HH: Humeral head; Gl: Glenoid.

1a. Rheumatoid arthritis

Early diagnosis of RA, which has a prevalence of about 1% in adults, is a challenge with huge potential benefit, before permanent disability is established [5]. RA is the commonest inflammatory arthropathy affecting the GHj, showing no specific clinical symptoms and signs [5, 7]. The GHj is involved in one third of patients with RA at the time of diagnosis [2]. Pathophysiologically, GHj involvement shares the same pattern with peripheral small joints. Synovial hypertrophy represents the cardinal feature which may harm the articular cartilage, subchondral and bare bone and periarticular soft tissues [6].

Radiographic abnormalities may be absent in 28% of patients with RA. However, they are usually evident in 45% and 64% of patients at 5 and 19 years from the onset of symptoms [8, 9]. In addition, RC symptomatology,

Inflammatory	Rheumatoid arthritis Seronegative arthropathies
Infectious	Septic arthritis
Crystalline arthropathies	HADD CPPD Gout
Neurological	Syringomyelia Erb's disease Parkinson
Avascular necrosis	Toxic (corticosteroids, alcohol abuse or radiation) Haemoglobinopathies Metabolic diseases (Gaucher's etc)
Miscellaneous	PVNS Amyloid arthropathy Synovial osteochondromatosis Haemophilic arthropathy
Traumatic	Trauma leading to macroinstability Overuse leading to microinstability Post-traumatic osteonecrosis of the humeral head
Postsurgical	Material failure or malposition Chondrolysis Altered biomechanics after capsulorrhaphy
Degenerative	Arthropathy caused by displacement of the humeral head after a rotator cuff tear

with or without a tendon tear, is present in up to 75% of patients with GHJ RA [9]. The earliest PR findings include soft tissue swelling and periarticular osteopaenia. Evolution of marginal erosions on the superolateral surface of the humeral head and in the medial aspect of the surgical neck of the humerus typically develop within 1-2 years from the onset of symptoms. Erosions of the articular surfaces and joint space narrowing (JSN) represent common end-stage findings [6, 8, 10-13].

The reported sensitivity of US, being similar to MRI, is better than PR regarding the detection of early erosions in the humeral head [8, 10-15]. In this context, US is superb in detecting early cortical erosions located at the superolateral aspect of the humeral head whereas MRI can better assess lesions located at the posterolateral cortex [13, 14]. Regarding synovitis, it can be accessed via US mainly by examining two locations, namely the posterior and axillary recess [16]. Synovitis is depicted as hypoechoic (infrequently isoechoic or hyperechoic)

relative to subcutaneous fat intraarticular tissue that is non-displaceable and poorly compressible with potentially concomitant effusion (**Fig. 1a**) [17]. Presence of synovitis should prompt the use of power or colour Doppler US to establish vascularity and, hence, inflammation of the tissue (**Fig. 1b**). Bursitis and tenosynovitis of the long head of biceps tendon, being present in a significant percentage of patients, can also be depicted by US. Hypoechoic or anechoic thickened tissue with/ out fluid within the tendon sheath, which is seen in two perpendicular planes and which may exhibit Doppler signal, defines tenosynovitis on US [17]. Distention of the subacromial-subdeltoid bursa due to synovial thickening (>3 mm) with/ out effusion represent US findings suggestive of bursitis [16].

Computed tomography (CT) has a limited role in RA of the shoulder. The method is utilised mainly for assessing the osseous structures for the presence of large erosions and JSN, when operative treatment is concerned [12].

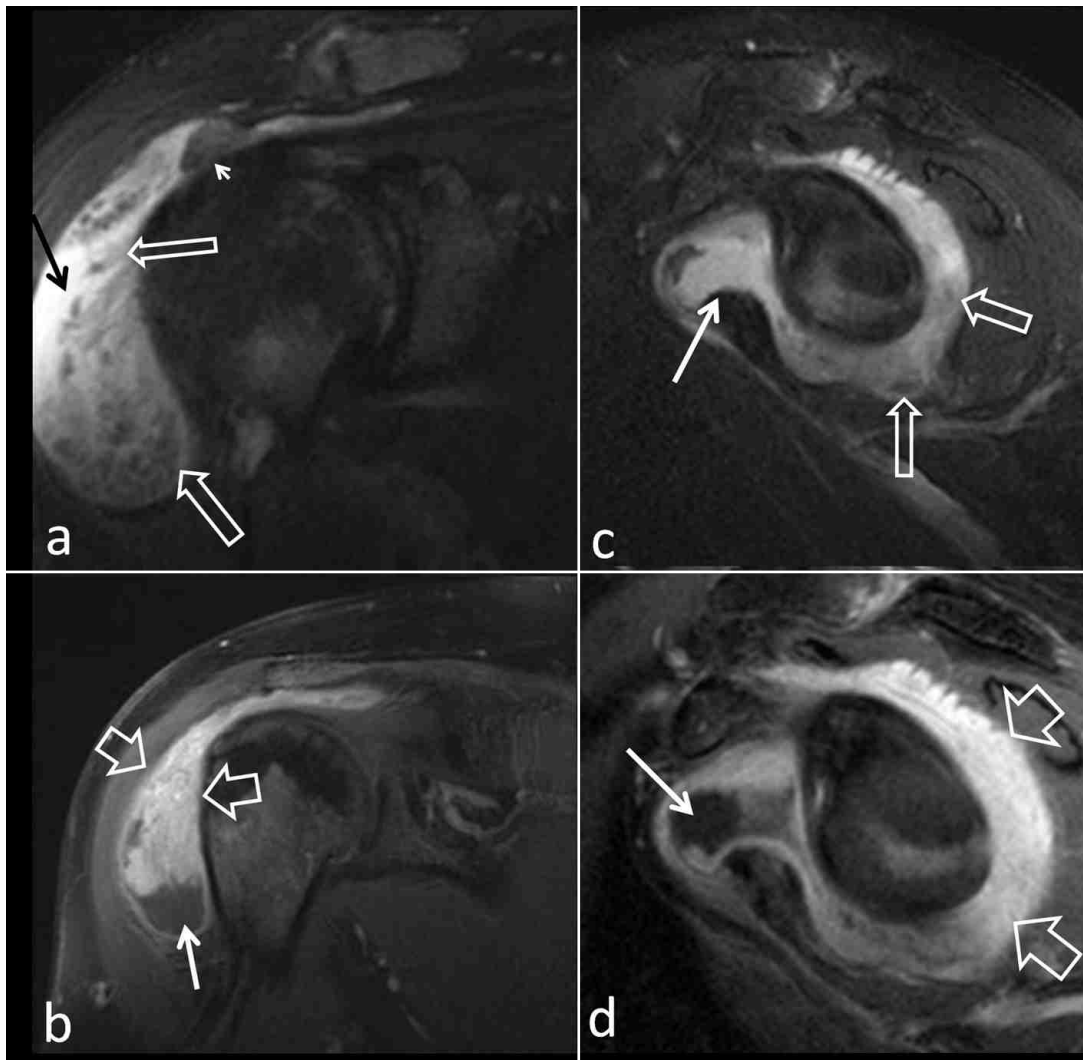


Fig. 2. A 49-year-old female patient with known rheumatoid arthritis of the wrists for 8 years and the left shoulder for 6 years. The oblique fat suppressed T2-w coronal (a) and fat suppressed contrast enhanced T1-w (b) MR images of the right shoulder show the joint effusion (thin arrows), the rice bodies (open thin arrows), the supraspinatus tendon tear with proximal retraction (arrowhead) and the extensive synovitis within the subacromial-subdeltoid bursa (open arrows). Bone marrow hyperplasia is the result of known iron deficiency anaemia. Early rheumatoid arthritis in the right shoulder of a 60-year-old female patient. The oblique sagittal fat suppressed T2-w (c) and fat suppressed contrast enhanced T1-w (d) MR images show the joint effusion (thin arrows), the synovial thickening with rice bodies (thin open arrows), and the extensive synovitis (open arrows).

MRI is the gold standard for the evaluation of intra-articular structures and bone marrow [13, 14]. Regarding synovitis, it is depicted as hypertrophied synovium, surrounding a joint effusion, which may enhance avidly after intravenous gadolinium administration (Figs. 1-3). With administration of intravenous contrast agents, MRI can differentiate synovial fluid from synovitis, as well as between hypervascular-active and fibrotic-inactive pannus [18]. The synovial proliferation leads to hypertrophied synovial villi

which may detach into the joint space or subacromial bursa and have an appearance of grains of rice and are called “rice bodies” (Figs. 1, 2) [5]. They typically show low to intermediate signal on T1W and low signal on T2W sequences [5]. Following intravenous contrast administration, they usually do not show enhancement [6]. Erosive changes are depicted as well-defined T2-hyperintense and T1-hypointense osseous lesions that communicate with the joint, often located at the posterolateral surface of the humeral head [2]. Bone

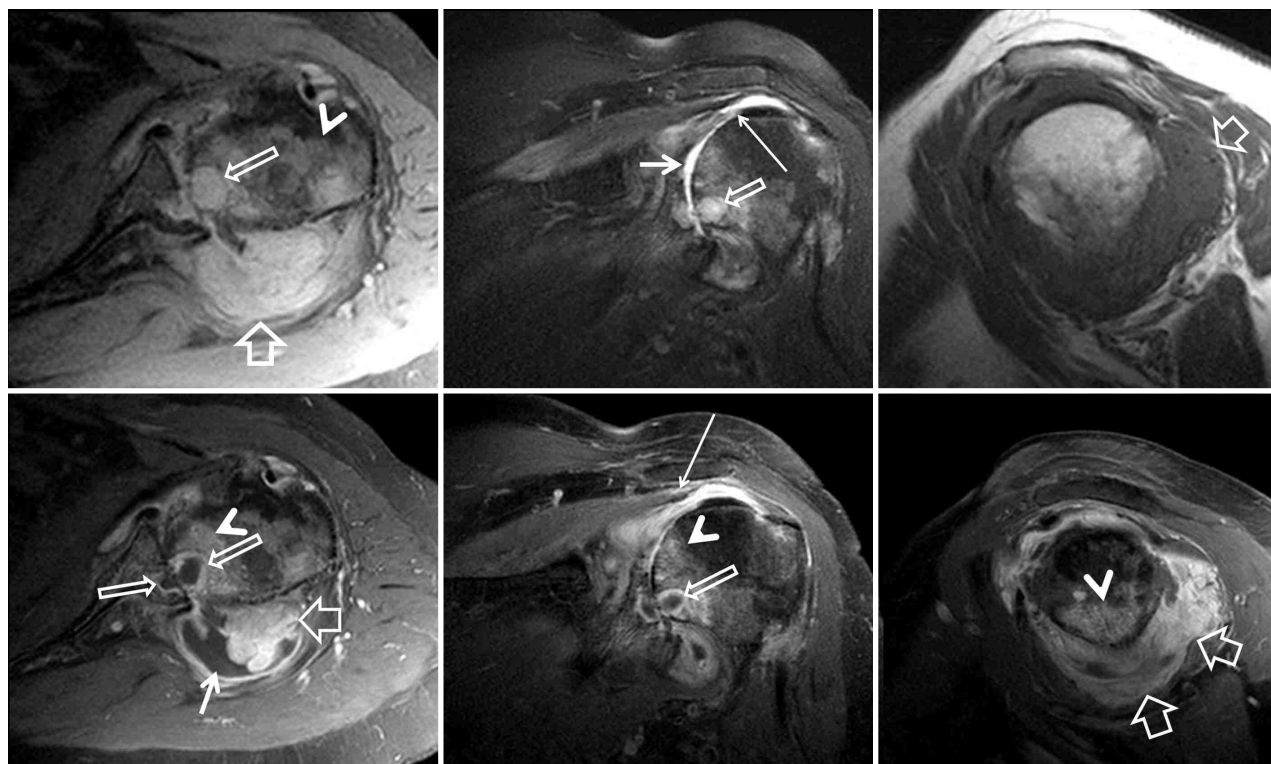


Fig. 3. Advanced rheumatoid arthritis of the left shoulder in a 70-year-old female patient. Upper row from left to right: axial fat suppressed PD-w, fat suppressed oblique coronal T2-w and oblique sagittal T1-w MR images. Lower row from left to right: fat suppressed contrast enhanced T1-w axial, oblique coronal and oblique sagittal MR images. Joint effusion (thin arrows), synovitis (open arrows), bone marrow oedema (arrowheads), erosions on both sides of the joint (thin open arrows) and supraspinatus and infraspinatus tears (long thin arrows) are shown.

marrow oedema (BME) in patients with RA is considered to be an early marker of inflammation [18]. BME is usually seen in subchondral locations or surrounding bone erosions and its presence is strongly related to the degree of synovitis and subsequent erosive damage [19]. Although approximately half of the patients with BME are going to develop erosions within one year, the altered marrow signal can be a potentially reversible feature [19]. RC abnormalities range from fraying to full-thickness tears and are commonly observed in patients with RA. Subsequent cephalad subluxation of the humeral head may be seen in patients with RC insufficiency [4, 7]. Adhesive capsulitis is the result of limited range of motion, secondary to chronic shoulder pain. In the era of advanced MRI techniques, perfusion MRI has been shown to represent a powerful tool for assessing response to treatment by applying quantitative evaluation of the contrast enhancement of the inflamed synovium. Hyaline cartilage degradation in RA

studied by newer MRI techniques and ultrahigh field MR scanners are currently under development [2].

1b. Seronegative arthropathies

SpA represent the second most common group of inflammatory arthritis, affecting about 0.6 to 1.9% of the European population [5]. Among all entities described under the term “SpA”, psoriatic arthritis (PsA), and ankylosing spondylitis (AS) most commonly affect the shoulder, with a reported incidence of up to 35% [20]. Shoulder is the second commonest extra-axial site of involvement in AS [6]. Inflammatory changes located at the tendinous, ligamentous and joint capsular insertions, called enthesitis, constitute the hallmark of SpA involvement. During the disease course, enthesitis may evolve into erosions and reactive bone formation, described as enthesophytes.

Although SpA shares many radiographic abnormalities with RA, the presence of bony proliferation and an-

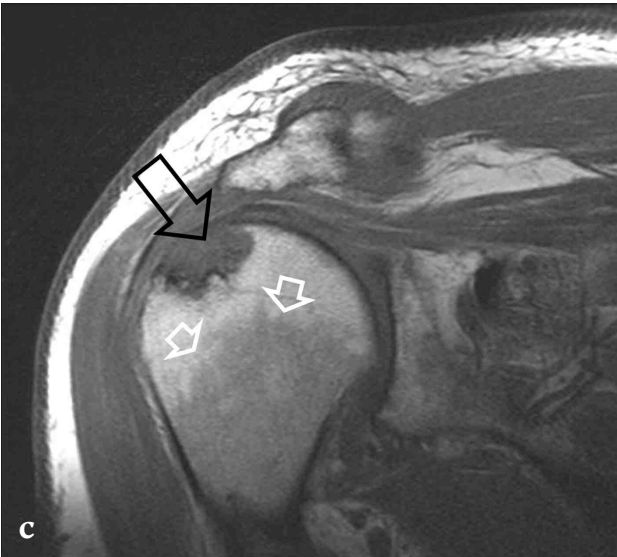
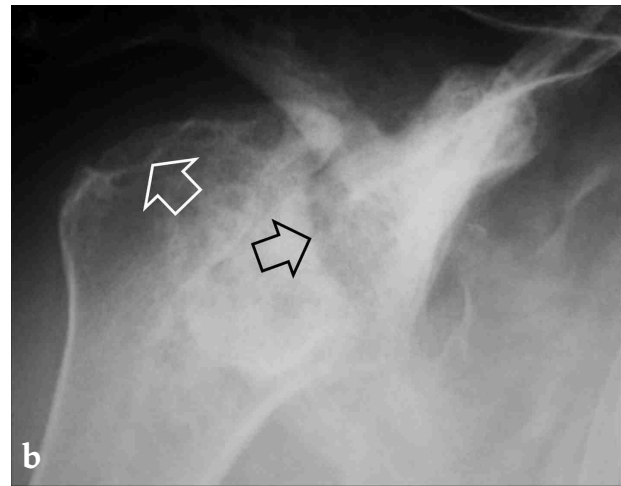
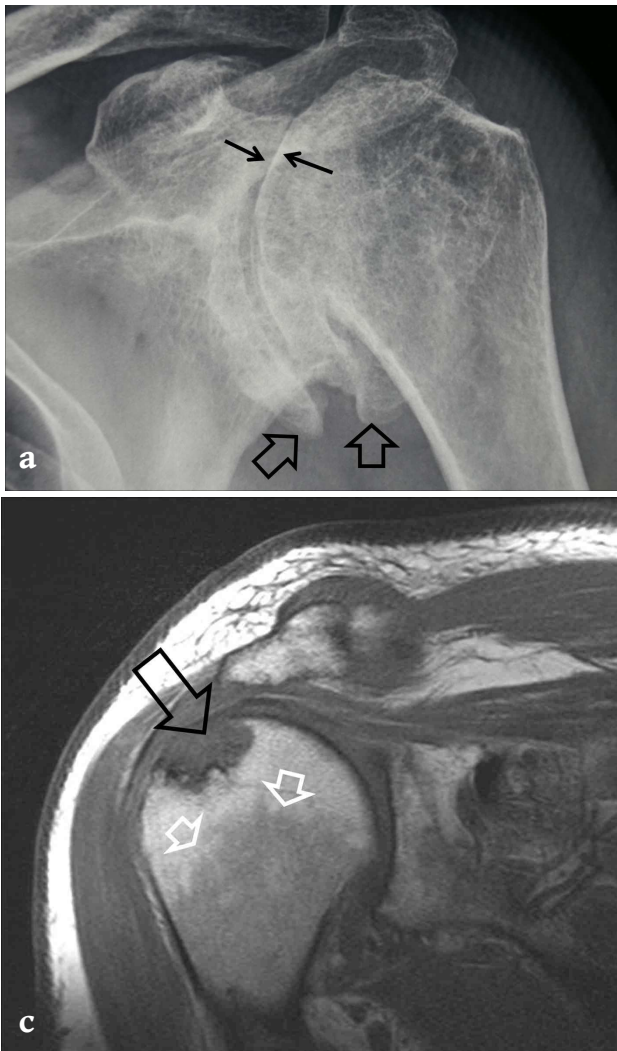


Fig. 4. a. A 70-year-old male patient with a history of psoriasis for the last 34 years and of axial spondyloarthritis for the last 22 years. The plain AP radiograph shows destructive osteoarthritis with joint space narrowing (thin arrows) and new bone formation (open arrows) secondary to psoriatic involvement of the glenohumeral joint. **b.** The plain AP radiograph of a 66-year-old male patient with long standing ankylosing spondylitis shows large erosions superolaterally (white arrow) and medially (black arrow). **c.** The oblique coronal T1W MR image in a 74-year-old male patient with long standing ankylosing spondylitis shows a large erosion on the superolateral humeral head (“hatchet” sign) (large arrow). Benign bone marrow hyperplasia (small open arrows) is the result of chronic anaemia.

kyloses serve as discriminating features between these two entities [6]. PR findings in the shoulder include JSN and the typical “hatchet sign”, which describes the presence of large erosion on the superolateral aspect of the humeral head (**Fig. 4**). Common MRI findings are subacromial bursitis, RC tendon tears with subsequent muscle atrophy and BME in the enthesal sites of the acromion and greater tubercle, with the latter carrying high specificity [4, 20]. US findings include swelling and neovascularisation at the enthesal sites. The presence of enthesitis at the insertion of the coraco-acromial ligament may result in enthesophytes leading to a “bearded acromion” [21]. Entesophytes may also develop at the acromial insertion of the deltoid, producing symptoms similar to those caused by impingement, particularly in patients with PsA [21].

1c. Juvenile idiopathic arthritis

Juvenile idiopathic arthritis (JIA) is the most common chronic disease in the paediatric population [22]. Shoulder involvement is seen late in the course of the polyarticular pattern of JIA, with a reported incidence of about 13% at 15 years after diagnosis [23]. Imaging investigation in JIA has a triple role: to increase clinical diagnostic confidence, detect potential complications related to the condition and to evaluate response to treatment [23]. MRI findings in JIA are similar to RA [23]. Care should be taken to obtain contrast enhanced images within 5 min following IV injection, as on late images there is a risk of over-diagnosing synovial inflammation, due to the diffusion of the contrast medium into the joint space [24, 25].

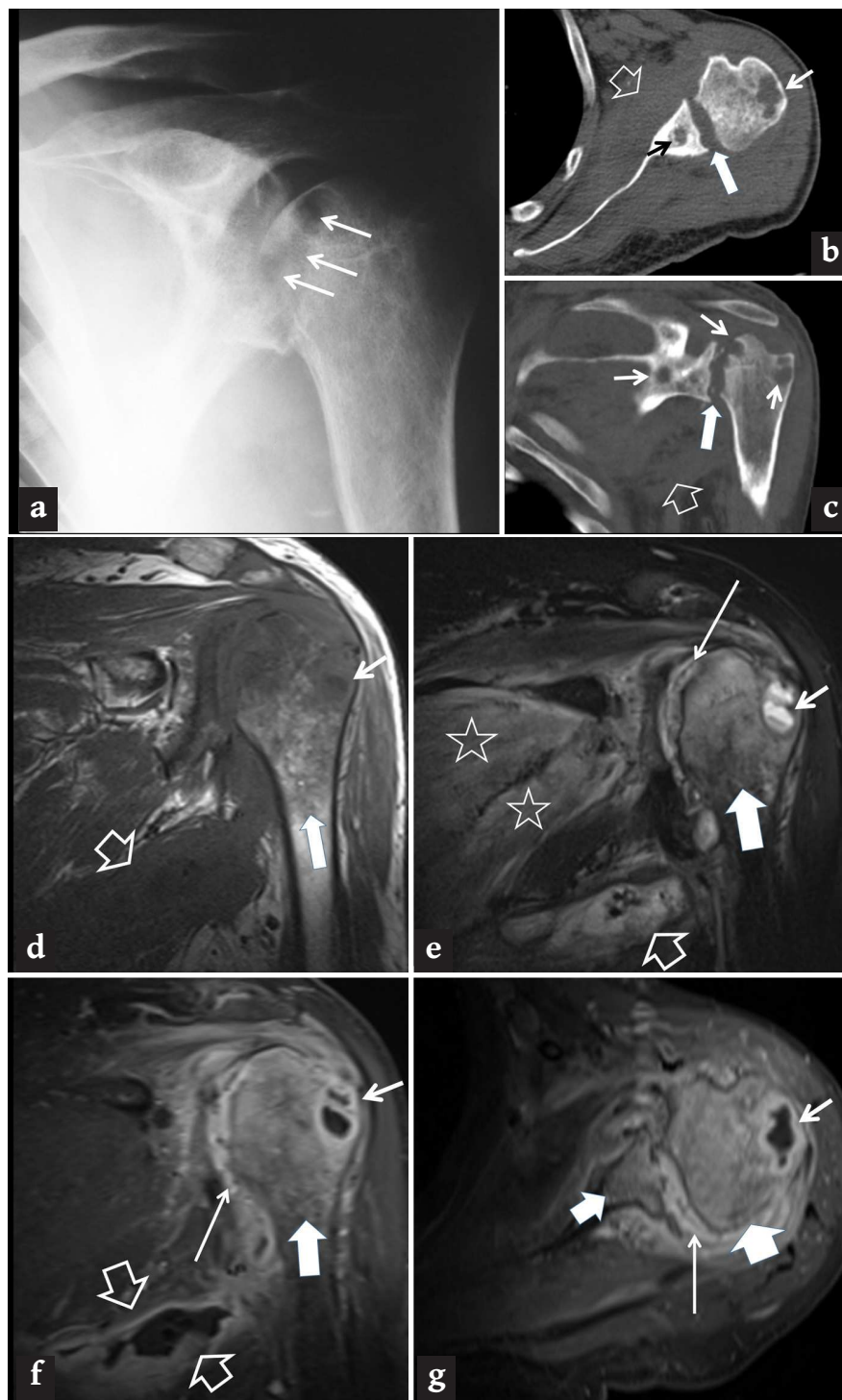


Fig. 5. Shoulder septic arthritis and osteomyelitis in a 72-year-old male patient, 3 months after genitourinary *Staphylococcus aureus* infection and shoulder pain of 3 weeks duration. **a.** AP radiographs shows osteolytic lesions in the medial aspect of the humeral head (arrows). Axial **(b)** and oblique coronal reconstruction **(c)** CT images show to better advantage the osteolytic lesions in both the glene and the humeral head (arrows) and cortical demineralisation of the intraarticular cortex with irregular articular surfaces (thick arrows). In addition, there is loss of fat planes and a lesion in the axillary cavity (open arrows). The oblique coronal T1W **(d)**, fat suppressed T2W **(e)**, contrast enhanced fat suppressed T1W **(f)** and contrast enhanced fat suppressed axial T1W **(g)** MR images show osteomyelitis (thick arrows), intraosseous abscesses (short arrows), joint effusion with synovial enhancement (long thin arrows) and soft tissue abscess (open arrows). Muscular oedema is also shown (stars).

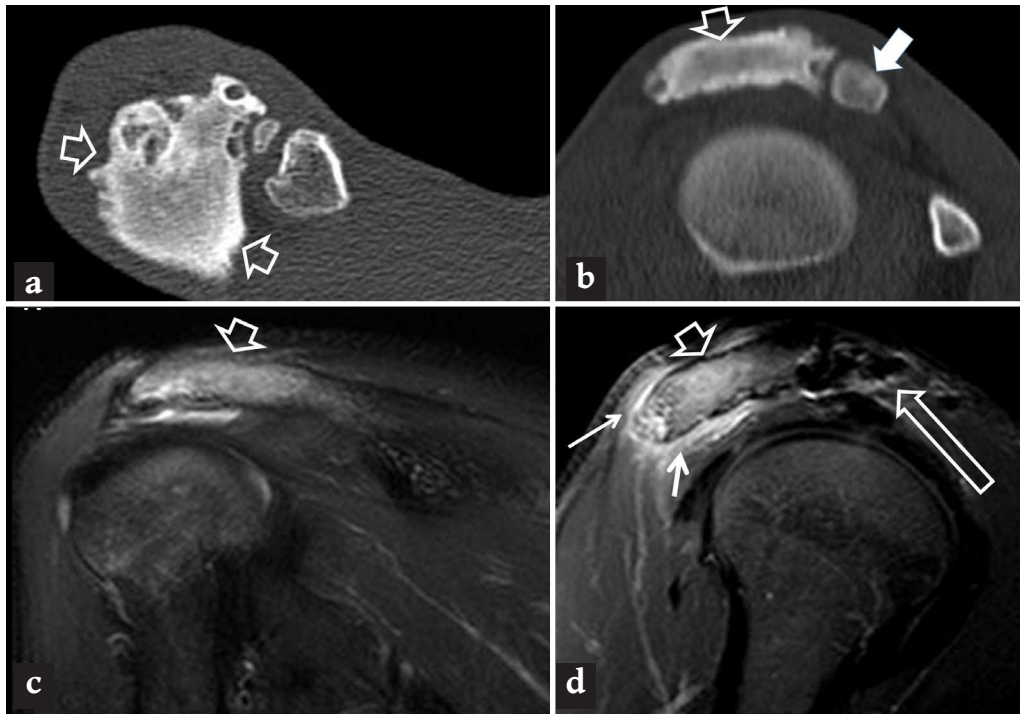


Fig. 6. A 30-year-old female patient with a history of acromioplasty 7 years ago, because of impingement due to os acromiale, complains of constant deep dull pain. Axial (a) and oblique sagittal reconstruction (b) CT images show marrow sclerosis and expansion of the acromion together with the irregular surface (open arrows). Fat suppressed oblique coronal T2W (c) and oblique sagittal contrast-enhanced T1W (d) MR images show bone marrow oedema and enhancement (open arrows) and reactive soft tissue oedema and enhancement (arrows). Note the remaining os acromiale (thick arrow in b) and susceptibility artefacts (long open arrow) due to the previous operation. Chronic sclerosing osteomyelitis was established with biopsy.

2. Septic arthritis

Shoulder is a rare site of septic arthritis in young adults. In one study, 18 cases were reported within 18 years [26]. Our own experience, excluding cases with total joint arthroplasty, is similar, with 5 confirmed cases within the last 9 years (unpublished data). However, it is becoming more common due to the increased number of arthroscopic and image-guided interventions [2]. Diagnostic injection for arthrography seems not to be related with septic arthritis because the injected contrast is bacteriostatic [6]. Most of the patients have an age of >60 years and usually have underlying systemic immunocompromised conditions such as diabetes, cirrhosis, neoplasia, leukemia and hypogammaglobulinaemia [26]. The presence of RA, gout, OA, intravenous drug abuse and steroid therapy are additional predisposing factors [6]. The prognosis is directly related to early diagnosis in an attempt to prevent complications, such as osteomyelitis, secondary OA and extension in the periarticular soft tissues [27, 28]. In this respect, im-

age-guided aspiration is important in order to isolate the responsible microorganism. It has been suggested that patients with culture negative infections, which may be seen in up to 47%, do have a better prognosis [29].

Staphylococcus aureus, which is isolated in about 40-70% of cases, represents the most common pathogen, followed by other Staphylococcus species and Gram-negative bacilli [26]. Mycobacterium tuberculosis (TB) is another pathogen with low virulence and insidious clinical course regarding joint involvement, which rarely involves the immunocompetent patients. Patients present with fever and malaise with restricted motion but in TB arthritis symptoms may be subtle for months. Serum CRP and ESR are usually elevated but peripheral WBC may be normal [2, 6].

Imaging is not used for diagnosis but rather to exclude other pathologies, to appreciate the extent of the disease and to reveal possible complications, such as abscess formation contributing to treatment planning [6].



Fig. 7. Hydroxyapatite deposition disease (HADD). Plain radiographs show extensive calcification in the supraspinatus of a 55-year-old female patient (arrows in **a**) with significant reduction 22 weeks after US-guided irrigation (arrow in **b**). **c.** A 42-year-old male patient with supraspinatus calcification (open arrows) and intraosseous extension (arrow). **d.** Fat suppressed MR images. Left, oblique coronal MR image showing round calcification over the infraspinatus tendon (open arrow) with soft tissue oedema (arrow) in a 61-year-old female patient. Center, axial MR image in 41-year-old female patient show calcifications on the infraspinatus tendon (open arrow) with intraosseous extension (arrow). Right, oblique sagittal MR image in a 28-year-old male patient show infraspinatus calcification (open arrow) extending into the bone with surrounding oedema (arrow) and into the subdeltoid bursa (thick arrow). **e.** Classification of calcific deposits based on their sonographic appearance. Left, hard calcifications depicted as two confluent hyperechoic rims (arrows) with posterior acoustic shadowing (asterisks) affecting the supraspinatus tendon in a 42-year-old female patient. Center, A 40-year-old female patient presenting with a soft calcification at the insertional portion of the supraspinatus tendon, depicted as a well-circumscribed, hyperechoic formation (arrows) without posterior shadowing. Right, A 52-year-old female patient with a fluid calcification located in the supraspinatus tendon, characterised by a hypoechoic center (asterisk), surrounded by a thin hyperechoic rim (arrows). S, supraspinatus tendon; HH, humeral head; B, biceps tendon.

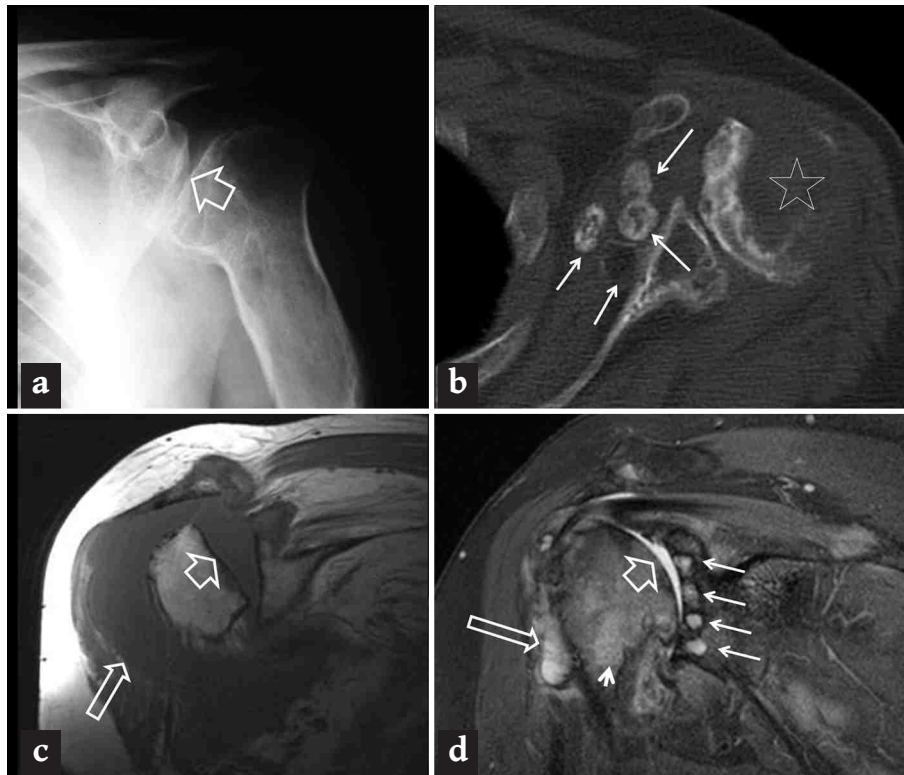


Fig. 8. “Milwaukee” shoulder. **a.** AP radiograph in a 82-year-old female patient showing the remodelling-“amputation” of the medial humeral head (arrow). **b.** Axial CT in a 78-year-old female patient showing the fragmentation of the humeral head (star) and multiple chondral and osteochondral loose bodies (arrows). A 77-year-old female patient with chronic poor function of the right shoulder. **c.** Oblique coronal T1W MR image showing the bone remodelling of the humeral head (short arrow) and the large effusion (long arrow). **d.** Fat suppressed PDW MR image showing effusion (long open arrow), bone remodelling (short open arrow), subchondral cysts in the glene (arrows) and bone marrow oedema (arrowhead).

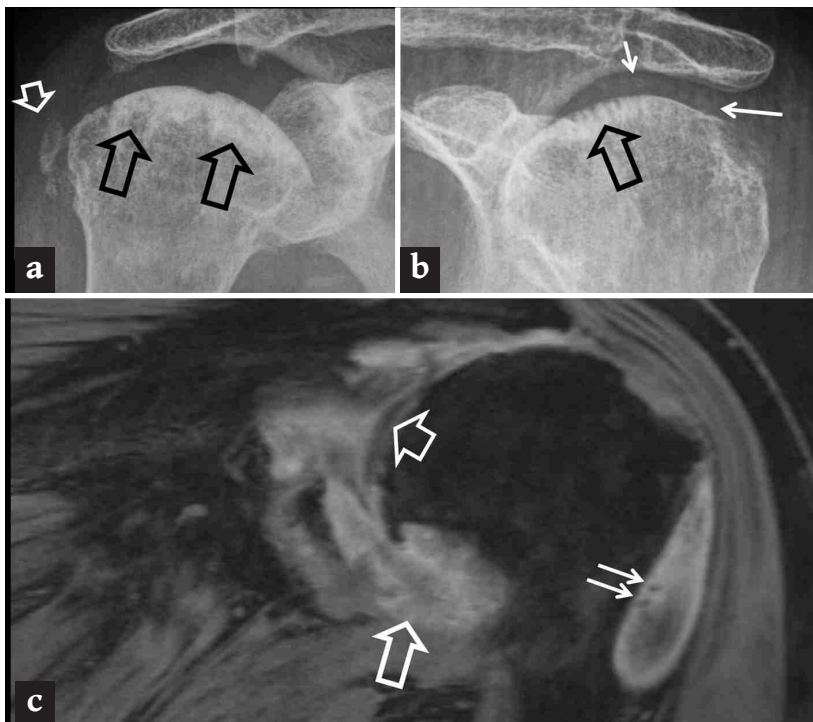


Fig. 9. CPPD in a 82-year-old female patient. AP radiographs in both shoulders (**a, b**) showing soft tissue calcifications (short open arrow), subchondral sclerosis (open arrows) and chondrocalcinosis (thin arrows on **b**). **c.** Oblique coronal fat suppressed T2* MR image showing chondrocalcinosis (short open arrow), effusion and synovitis (open arrow) and small intrabursal calcifications (thin arrows).

In the acute phase of septic arthritis, PR may be normal or show non-specific findings such as joint effusion and periarticular osteopaenia. As the disease progresses, joint space narrowing, marginal erosive changes and osteomyelitis of the bones involved become apparent (**Fig. 5**) [2]. US has an evolving role in the overall handling of the disease by showing effusion, non-compressible synovial hypertrophy and often Doppler signal [30]. Diagnostic aspiration may be performed on the same session. CT shows to better advantage the osteomyelitis complicating septic arthritis (**Fig. 5**). In addition, chronic osteomyelitis is shown with bone expansion and osteosclerosis (**Fig. 6**).

MRI abnormalities in the septic joint have been described to be present as early as 24 hours after the onset of symptoms [31]. MRI is the imaging modality of choice mainly because it allows for early clinical confirmation and detection of coexisting osteomyelitis in the humerus and/or glenoid, a feature which may raise the need for alteration of the therapeutic approach. MRI also offers the advantage of depiction of the infection's extent in the surrounding soft tissues and safely excludes other possible pathologies. Early MRI findings are non-specific and include synovial enhancement, perisynovial oedema, joint effusion and BME, yet 30% of patients with septic arthritis may lack an effusion [2, 28]. Synovial inflammation, joint effusion and BME are better shown on fluid sensitive sequences. T1W and fat suppressed contrast-enhanced T1W images are useful in the detection of synovitis and osteomyelitis (**Fig. 5**) [27]. Contrast-enhanced images are particularly sensitive in differentiating abscesses from surrounding cellulitis and/or myositis [28]. Persistent foci of fatty signal within bone marrow have been suggested to represent a frequent finding in acute osteomyelitis [32]. In more advanced cases, the synovial inflammation disrupts the cartilage and cortical bone, especially of the bare areas and causes erosions and JSN, potentially within days from the onset of symptoms. None of the above features is diagnostic of septic arthritis, although erosions in conjunction with BME are highly indicative [2]. MRI can be used to monitor the treatment response in proven and treated septic arthritis. Reduced size of abscess or joint effusion suggest response. Synovial thickness and enhancement, periarticular myositis or cellulitis and BME may persist for long [29].

In the postoperative setting, MRI has limitations due

to metal artefacts and determination of active disease may be challenging. A variety of technical modifications, such as the use of STIR instead of spectral fat suppression and smaller voxels, as well as the avoidance of gradient echo sequences, can improve the quality of the images.

3. Crystal-induced arthropathies

3a. Hydroxyapatite deposition disease

Hydroxyapatite deposition disease (HADD) or calcific tendinopathy is characterised by the deposition of calcium hydroxyapatite crystals in the RC tendons, the peritendinous soft-tissues, subacromial-subdeltoid bursa or the underlying humeral head, giving rise to “intraosseous HADD” (**Fig. 7**) [5, 33-40]. The disease shows a preference for the shoulder joint, with supraspinatus tendon being the most common location [34, 41, 42]. HADD is a common arthropathy affecting mainly women aged between 30 and 60 years [42, 43]. Although its aetiology remains unclear, the calcific depositions seem to evolve through three stages, namely the precalcific, the calcific (which is further classified into formative and resorptive) and finally the postcalcific [34]. Despite the usually self-limiting nature of the condition, intense and highly disabling pain may occur especially during the calcific stage, particularly at the resorptive phase. PR may detect the presence of calcifications in the soft tissues around the humerus with variable shapes and sizes (**Fig. 7**) [35]. Three types have been described: (i) type I, well circumscribed and dense, corresponding to the formative phase; (ii) type II: well circumscribed and inhomogeneous or homogeneous with no defined border; and type III; translucent and cloudy without sharp outline, corresponding to the resorptive phase (**Fig. 7**) [36, 37, 42].

On US, the calcium deposits usually appear hyperechoic with/out posterior acoustic shadowing and various classifications systems have been proposed [44]. Three different calcifications types have been described according to the percentage of containing calcium. In type I, calcifications appear as hyperechoic foci with associated strong acoustic shadowing. Type II calcification appears as hyperechoic foci with a mild acoustic shadow while type III lesions are depicted isoechoic to the tendon and lack acoustic shadow [45]. Type I corresponds to the formative phase while type II and III calcifications correspond to the resorptive phase [45].

Additionally, the value of colour Doppler in identifying lesions in the formative and resorptive phase as well as correlation between colour Doppler findings and clinical symptoms has been reported [46].

MRI may show the low signal intensity of the calcifications on all pulse sequences. However, lesions may remain occult on conventional MRI [47]. In this scenario, susceptibility-weighted imaging may be of value in identifying calcific deposits with a sensitivity of 98% and specificity of 96% when compared to radiography [40]. Surrounding oedema suggests inflammation (resorptive phase) [37]. No correlations appear to exist with subacromial impingement according to one study [48]. MRI is particularly useful for assessing the potential intraosseous migration of calcifications, by determining connection between the osseous and soft tissue calcific component. Thus, clarification versus an aggressive neoplastic lesion is usually feasible (**Fig. 7**) [38, 39, 49].

3b. Milwaukee shoulder

A specific pattern, resulting from the presence of calcium hydroxyapatite crystals into the GHJ, is the “Milwaukee shoulder” which leads to rapid destruction of the joint [50]. “Milwaukee shoulder” is more prevalent in elderly women, often with bilateral involvement (>80%) [51]. It presents with pain, limited range of motion and swelling. PR show soft tissue oedema, JSN, subchondral sclerosis, destruction of the bony structures and fragmentation leading to typically large intra-articular loose bodies. Common MRI findings include RC tears, marked joint effusion, destruction of the articular surfaces with cartilage thinning and subchondral cysts, multiple osteochondral loose bodies and synovial proliferation (**Fig. 8**) [4].

3c. Gout

Gout is a common crystalline arthropathy that rarely affects the shoulder, usually in the polyarticular disease pattern [15]. It primarily affects men in their 5th-7th decades of life [4]. Pathogenesis relates to deposition of monosodium urate crystals, leading to an inflammatory response which in the acute phase can mimic septic arthritis. In the acute phase, radiological findings are non-specific, showing soft tissue swelling and joint effusion. In untreated patients the disease proceeds to a chronic phase, with the characteristic presence of

tophi, which represent bulky monosodium urate deposits in subcutaneous, periarticular or intraarticular soft tissues [15]. PR in chronic disease show iso- or hyperdense soft tissue or intraosseous tophi, new bone formation and paraarticular erosions with overhanging edges, with preservation of the joint space [51, 52]. CT utilising the dual energy technique with bone algorithm and 3D reconstruction, can automatically evaluate the amount of urate crystals, detect occult to PR or MRI erosions and monitor response to treatment [53]. Thus, CT currently has significantly reduced the rate of diagnostic aspiration of a joint and has been included in the widely used classification system [54]. On MRI tophi are of various signal intensity, mostly iso- to hypointense on T1W and intermediate to low signal on T2W MR images. Intravenous contrast administration shows homogeneous enhancement [5, 35]. US shows synovitis and hyperaemia in the acute phase and hyperechoic crystal aggregates of the soft tissues in the chronic phase. A gout-specific US finding is the “double contour” sign, which shows high specificity (>0.98) for diagnosis [52, 55, 56]. In conclusion, the intra- and peri-articular inflammation matched with the joint space sparing and the extraarticular erosions, are suggesting the correct diagnosis.

3d. Calcium pyrophosphate deposition or Pseudogout disease

Calcium pyrophosphate deposition disease (CPPD) is characterised by deposition of calcium crystals in hyaline cartilage, fibrocartilage and periarticular soft tissues as well as in ligaments and tendons [15]. Chondrocalcinosis is seen in about 60% of individuals over 80 years, better depicted with CT, as incidental findings. Thus, “chondrocalcinosis” corresponds to the hyaline cartilage and fibrocartilage and soft tissue calcification whereas “pyrophosphate arthropathy” (PA) corresponds to the osseous and chondral complications resulting from the crystal deposition [57]. PA is more common in elderly women and may be clinically expressed with five different patterns, simulating distinct disorders [6, 58, 59].

CPPD may affect non weight-bearing joints, mainly in elderly patients, is related to OA, primary hyperparathyroidism and haemochromatosis and is commonly identified in the shoulder area. The disease’s clinical picture is variable and ranges from totally asymptomatic to acute flares, when the crystal deposits are re-

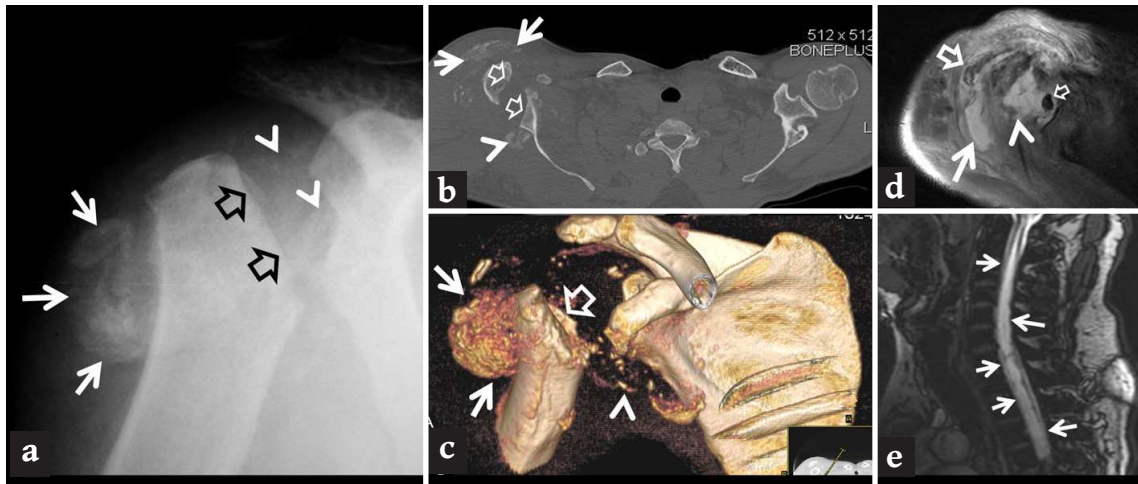


Fig. 10. A 32-year-old man presented right shoulder swelling and severe limitation of range of motion for the last 9 months. **a)** AP radiograph showing humeral head remodelling (open arrows), soft tissue ossification (arrows) and intraarticular “cloud” like loose bodies (arrowheads). **b)** Axial bone algorithm (**b**) and VRT reconstruction (**c**) showing to better advantage the humeral head and glenoid remodeling (open arrows), the ossified lesion within the subdeltoid bursa (arrows) and the intraarticular loose bodies (arrowheads). **d)** Axial fat suppressed PDW MR image showing bursal effusion (arrow) with the ossified lesion (open arrow), joint effusion (arrowhead) and necrotic bone debris into the joint (small open arrow). **e)** Sagittal T2* MR image showing extensive syringomyelia (arrows) which resulted in a neuropathic joint.

leased into the synovial fluid, causing an inflammatory response which can mimic gout, infection and RA. On PR and CT, chondrocalcinosis, striated calcifications of the tendons, subchondral cysts and sclerosis and considerable JSN are evident (**Fig. 9**). US findings typical for CPPD are synovial inflammation and hyperechoic deposits without acoustic shadowing [55]. MRI may miss the crystal deposition unless a T2* sequence is used (**Fig. 9**).

4. Neuropathic arthropathy

Neuropathic osteoarthropathy (NA) or Charcot’s arthropathy is a chronic and progressive disorder that is related to loss of deep sensation and proprioception, secondary to central or peripheral neurologic impairment [32, 50]. It has been described in cases of syringohydromyelia, meningomyelocoele, multiple sclerosis, trauma, diabetes mellitus, alcoholism, spinal tumours, amyloidosis and repeated corticosteroid injections [7, 35]. Regarding the shoulder, syringohydromyelia at the level of cervical spine, regardless of its primary cause, represents a common associated finding being observed in 75% of cases [60]. The symptoms are quite variable and include reduced range of motion, hypoaesthesia, swelling, muscle weakness and pain. Early findings on

PR resemble OA, which progresses rapidly within days or weeks. The atrophic findings are predominant, but in advanced cases massive osteolysis is identified, mainly on the humeral head but also on the glenoid. Remodelling of the humeral head with sharp “surgical” margins at the edge of the resorption is typical for NA, and is in contrast with the ill-defined borders that are seen in septic arthritis (**Fig. 10**) [4]. Other radiographic findings characteristic of advanced disease include fragmentation of the subchondral bone, intraarticular loose bodies, osteophyte formation, subluxation, effusion and periarticular fractures [5]. MRI shows degeneration of the rotator cuff tendons, joint effusion, BME and aggressive osseous destruction that may mimic malignancy [60, 61]. CT with 3D reconstruction, may show the extension of the destructive process (**Fig. 10**).

5. Avascular necrosis

The proximal humerus is the 2nd commonest site of avascular necrosis (AVN). The aetiology is most of the times related to systemic corticosteroid treatment. Alcohol abuse, chemotherapy/irradiation, systemic lupus erythematosus, pancreatitis, Gaucher’s disease, haematological diseases, extraarticular proximal humeral fracture fixation and Caisson’s disease are common rec-

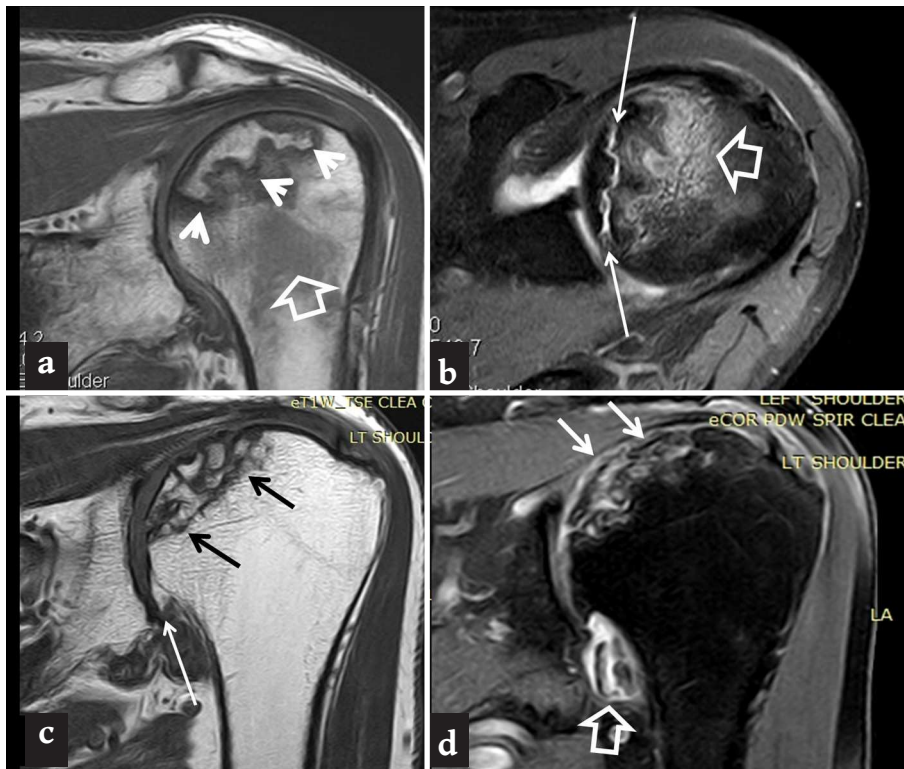


Fig. 11. A 60-year-old, previously healthy patient, presents with left shoulder pain. **a)** Oblique coronal T1W MR image showing the pathognomonic for osteonecrosis low signal intensity serpentine “band-like” sign (arrows). Low signal intensity poorly defined area in the metaphysis (open arrow) suggests bone marrow oedema. **b)** Axial fat suppressed PDW MR image showing the subchondral fracture (“crescent” sign) (thin arrows) and bone marrow oedema (open arrow). Oblique coronal T1W (**c**) and fat suppressed PDW (**d**) MR images 9 years later, with conservative treatment, showing fragmentation of the osteonecrotic area (arrows), osteoarthritic changes with joint space narrowing and osteophyte formation in the lower glenohumeral joint (long arrow) and small loose bodies in the axillary recess (open arrow).

ognised causes [5, 62]. In the shoulder area, AVN usually is asymptomatic, till collapse or arthrosis occur [62]. On PR, AVN of the humeral head in the early stages may be occult or appear as arc-like subchondral lucencies and sclerosis. As the disease advances, subchondral fracture (“crescent” sign) and cortical collapse may be seen, without GHJ JSN. MRI is the method of choice to detect AVN on an early stage by showing the pathognomonic serpentine low signal intensity zone on T1-w images, known as the “band-like” sign (**Fig. 11**). The “crescent” sign, which on MRI is a subchondral fracture, filled with fluid on fat suppressed images, suggests advanced disease. The presence of surrounding BME suggests articular surface collapse (**Fig. 11**).

6. Primary Osteoarthritis

Primary osteoarthritis (OA) of the shoulder is not as com-

mon as OA of the knee or hip which are weight-bearing joints. It has a prevalence at about 33% of the population older than 60-years-old and shows no predilection for dominant or non-dominant site. On PR, primary OA is diagnosed with true AP views of the shoulder, showing JSN with preservation of the subacromial space, subchondral sclerosis, cystic changes superomedially and osteophytes [63]. Loose bodies are seen in late stages of the disease. The humeral head may become flattened and posteriorly decentered forming a “neoglenoid” which is seen in axial radiographs as a biconcave glenoid surface [63]. Classification systems of primary OA are based on humeral osteophytes formation, humeral head sphericity and glenoid morphology [64].

6a. Rapidly destructive osteoarthritis

Rapidly destructive osteoarthritis (RDOA) represents a

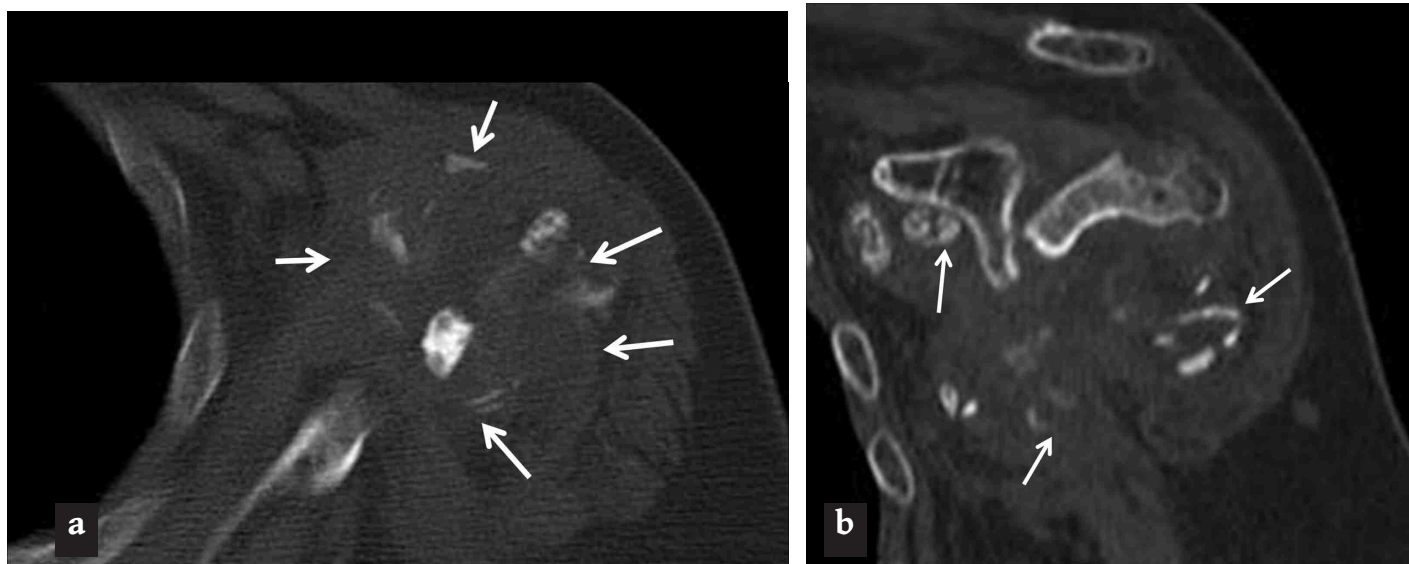


Fig. 12. Rapidly destructive osteoarthritis in a 72-year-old female patient. Axial (a) and oblique coronal (b) CT image in bone algorithm, shows fragmentation of the bony humeral head with some loose bodies located into the joint effusion (arrows).

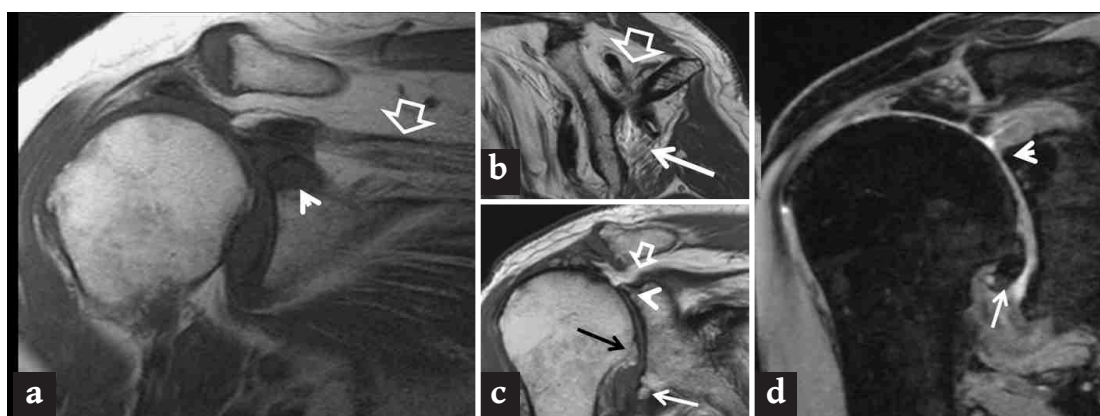


Fig. 13. Rotator cuff arthropathy. T1W oblique coronal (a) and oblique sagittal (b) MR images showing fatty infiltration of the supraspinatus muscle (open arrows) and infraspinatus muscle (long arrow). Subarticular cyst in the upper glene (arrowhead) corresponds to osteoarthritis. T1W (c) and 3D-T2* (d) oblique coronal MR images showing the torn and retracted supraspinatus tendon (open arrow), osteophyte formation (long arrows) and joint space narrowing (arrowheads). Cephalad migration of the humeral head is shown on all coronal images.

subset of OA which was initially described in the hip joint. RDOA may involve the GHJ, mostly in elderly women with a mean age of 72. In 13% of cases, patients have synchronous hip RDOA [65]. The lack of abnormal WBC count and CRP serum levels exclude infection as the underlying cause. The clinical and radiographic manifestation of RDOA can be dramatic and pose diagnostic challenge because advanced RA, septic arthritis, crystal-induced arthritis and NA may lead to similar imaging findings. The original definition of the RDOA in the hip included a joint

space loss of >50% within 1 year or a rate of joint space loss of >2 mm/year. An overlap with the previously described HADD-“Milwaukee” shoulder may exist [66]. The major radiological finding is the medial or superomedial flattening of the humeral articular surface [67]. Joint effusion, synovitis and BME in the humeral head can also be evident on MRI. Late radiological findings consist of destruction of the humeral head with intraarticular osseous debris and differential diagnosis with NA is required (Fig. 12) [58]. The treatment for RDOA is joint replacement [66].



Fig. 14. A 55-year-old female patient with proven PVNS. Oblique coronal fat suppressed T2W (**a**), T1W (**b**) and fat suppressed contrast enhanced T1W (**c**) MR images show joint effusion with low signal intensity structures in the axillary recess (arrows), moderately high signal intensity of the effusion due to blood (open arrow) and synovial enhancement with no enhancement of the low signal intensity structures (arrows in **c**) which correspond to haemosiderin. Supraspinatus tendon tear is also shown in **a** (arrowhead).

7. Rotator cuff tear arthropathy

Rotator cuff tear arthropathy (RCTA), first described in 1977 by Neer et al., is the result of disruption of the stabilising role of the RC in the hyper-mobile GHj. It is recognised by three distinct stages: a massive RC tear, degenerative joint changes and superior migration of the humeral head [68]. A massive tear is defined either with a gap of ≥ 5 cm or of complete tear of two or more tendons [69,70]. These changes inevitably result in instability of the GHj with superior migration of the humeral head leading to secondary OA. This has been described as “femoralisation” of the humerus and “acetabularisation” of the coracoacromial arch [71]. Imaging findings with PR, CT and MRI are those of degenerative OA (**Fig. 13**). PR show the superior migration of the femoral head, osteophytes formation, subchondral sclerosis, cystic lesions at the greater tuberosity and JSN [5]. Radiographically, the Hamada classification assesses the distance between the acromion and the humeral head for predicting the severity of RCTA [72]. Muscle atrophy and fatty infiltration can be assessed with MRI, using the Goutallier classification system. Fatty infiltration of more than 50% favours arthroplasty rather than tendon repair [69, 73].

8. Miscellaneous

8a. Capsulorrhaphy arthropathy

Capsulorrhaphy-related arthropathy is defined as the secondary OA following a previous surgical operation in the shoulder, i.e. RC repair and repair of any kind

of instability [74]. One of the pathomechanisms is the overtightening of the anterior capsule which forces the humeral head to sublux posteriorly. Clinical history together with features of OA typically located at the posterior GHj may imply the correct diagnosis.

8b. Amyloid arthropathy

The main pathogenetic pathway of the disease is the accumulation of $\beta 2$ -microglobulins in patients undergoing chronic haemodialysis. This low molecular weight serum protein is not filtered by the dialysis membranes [75]. Shoulder is the commonest symptomatic joint, usually showing bilateral involvement. The cervical spine is another common location. Patients may present with striking enlargement of both shoulders, known as the “shoulder pad” sign. Amyloid infiltration leads to soft tissue or well-defined lytic subchondral bone lesions called amyloidomas [35]. The affected bone is susceptible to pathologic fractures, which represent a common complication. PR show soft tissue swelling, osteopaenia and well-defined osteolytic lesions [35]. The joint space usually is spared until late in the disease course. On MRI, soft tissue amyloid depositions typically show low to intermediate signal intensity on both T1W and T2W images. Thickening of the RC tendons and synovium and joint and bursal effusions represent associated findings [5].

8c. Pigmented villonodular synovitis

Pigmented villonodular synovitis (PVNS) is a benign

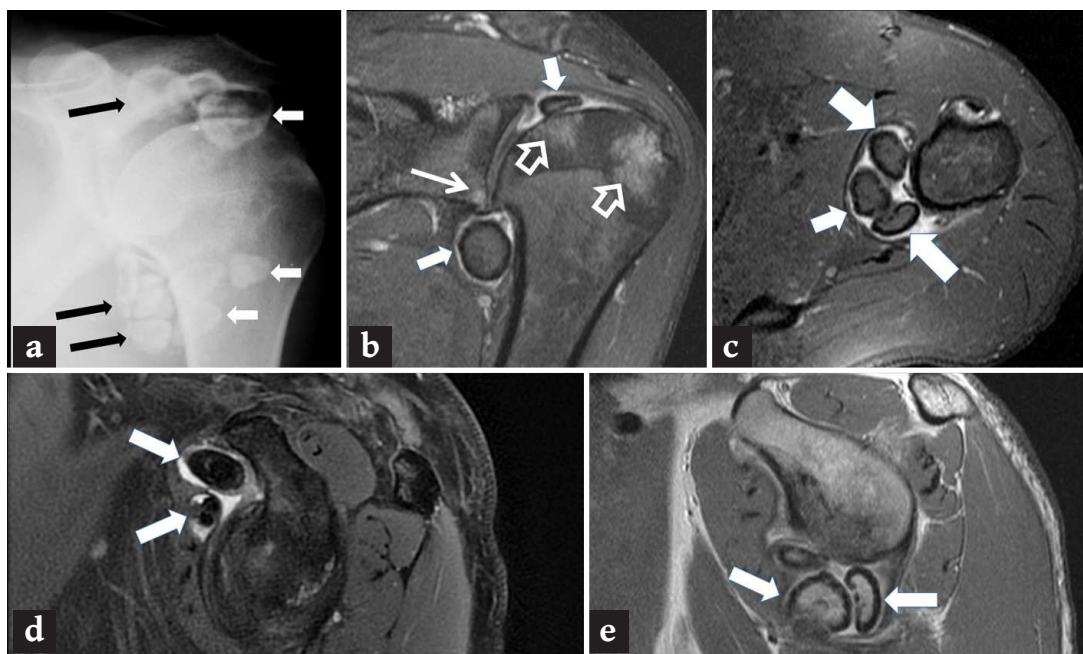


Fig. 15. A 42-year-old male with pain and “clicking” of his left shoulder for the last 8 years. AP radiograph (a) and fat suppressed PDW oblique coronal (b) and axial (c) MR images showing the multiple osteochondral loose bodies (thick arrows), joint effusion, reactive bone marrow oedema (open arrows) and early onset osteoarthritic changes in the lower glenohumeral joint (thin arrow). Fat suppressed PDW (d) and T1W (e) oblique sagittal MR images in two different patients showing the osteochondral loose bodies in the subcoracoid bursa and axillary recess (arrows).

proliferative disorder of the synovium, usually monoarticular, which can be diffuse or focal. In 80% of the cases the condition shows a predilection for the knee joint. Shoulder represents a very uncommon target, which is typically affected in older patients (3rd to 4th decade) than in other locations. The hallmark of this disease is the haemosiderin accumulation in the synovium, which appears thickened and hyperplastic. Early imaging findings on PR include periarticular osteopaenia and soft tissue swelling with characteristic preservation of the joint space. Juxtaarticular large bone erosions and JSN denote advanced disease. On CT erosions may be evident at an earlier stage. Haemosiderin deposits in the synovium may appear of high attenuation on both PR and CT. MRI is the imaging modality of choice, showing a thickened irregular synovium of low signal intensity on both T1W and T2W MR images, areas of fatty tissue that represent lipid laden macrophages and preserved joint space (Fig. 14) [76]. The low intensity lesions show the characteristic blooming artefact on gradient-echo images, owing to the paramagnetic properties of haemosiderin [4]. The differential diagnosis includes amyloid arthropathy, gout, haemophilia, RA and synovial

osteochondromatosis [35]. Susceptibility artefacts and monoarticular involvement can discriminate PVNS from the other disorders [5].

8d. Synovial (osteo)chondromatosis

Primary synovial chondromatosis or "Reichel-Jones-Henderson" syndrome is a benign monoarthropathy characterised by synovial metaplasia and formation of multiple chondral or osteochondral loose bodies. Men are affected twice more frequently than women. Owing to their intraarticular location, loose bodies are associated with the development of secondary OA due to entrapment and friction, although they can also be found in bursae and tendon sheaths [4, 77]. The exact pathomechanism remains unknown. Secondary osteochondromatosis is associated with trauma, OA, AVN and NA, and in such cases the intraarticular nodules are less in number, larger and of varied size compared to those in primary osteochondromatosis [4].

Radiologically, the findings are variable and mirror the amount of calcification in the cartilaginous nodules. The cardinal feature is the presence of numerous, small, well-circumscribed loose bodies into the joint space. Os-

sification of the nodules is present in about 70% to 75%. PR in chondromatosis may be normal or show non-specific findings such as soft tissue lesions that surround or even widen the joint. Erosive and early OA changes denote advanced disease. In osteochondromatosis, the radio opacity of the nodules can easily suggest the diagnosis (**Fig. 15**) [4]. CT may show the loose bodies to better advantage. MRI can depict the intraarticular formations, especially in the presence of concomitant joint effusion. The signal intensity depends on the degree of cortication and presence of mature marrow within the chondral bodies (**Fig. 15**).

8e. Haemophilic arthropathy

Haemophilic arthropathy (HA) represents a complication of haemophilia A (classic haemophilia) or haemophilia B (Christmas disease), occurring commonly during the 1st or 2nd decade of life. Shoulder is the 4th most common site of involvement in HA, after knee, ankle and elbow. The pathophysiology involves recurrent episodes of intraarticular bleeding, with subsequent inflammation, synovial hyperplasia, fibrosis, and iron deposition [4]. Radiographic findings are related to the stage of the disease, which can be divided in five levels of severity: haemarthrosis, synovial inflammation and hyperaemia, chondral erosions and subchondral resorption, cartilaginous degeneration and joint disorganisation with intraosseous and subperiosteal haemorrhage, along with bony proliferation [5]. The PR findings depend upon the stage of the disease. Initially, there is joint effusion with periarticular osteoporosis. Later on, epiphyseal enlargement and joint space narrowing with subchondral cysts are seen. Typically in the knee, there is widening of the intercondylar notch and flattened condylar surfaces along with squared inferior

patellar pole. The synovium usually shows low intensity on MRI, producing also a susceptibility artefact due to haemosiderin deposition on gradient echo pulse sequences. The subchondral erosive changes may be of high (fluid), intermediate (fibrous) or low (haemosiderin) signal on T2W images [5].

Conclusion

In this pictorial essay we highlighted the most common arthropathies affecting the shoulder from an imaging perspective. In the acute clinical setting, inflammatory, crystal induced arthropathies and infections should be initially considered. In patients with chronic symptoms, OA, AVN, RC arthropathy and NA are mainly included in the differential diagnosis. Familiarity with the multi-modality imaging appearance of these entities is of utmost importance for achieving a timely and accurate diagnosis. **R**

Funding

This project did not receive any specific funding.

Conflict of interest

The authors declared no conflicts of interest.

Abbreviations: PR: plain radiographs; US: ultrasonography; CT: computed tomography; RC: rotator cuff; MRI: magnetic resonance imaging; JSN: Joint space narrowing; GHj: glenohumeral joint; ACj: acromioclavicular joint; BME: bone marrow oedema; RA: rheumatoid arthritis; SpA: seronegative spondylarthropathies; PsA: Psoriatic arthritis, AS: ankylosing spondylitis, JIA: Juvenile idiopathic arthritis; CPPD: calcium pyrophosphate deposition disease, PA: pyrophosphate arthropathy, NA: neuropathic arthropathy; PVNS: pigmented villonodular synovitis

REFERENCES

1. Armstrong A. Evaluation and management of adult shoulder pain: a focus on rotator cuff disorders, acromioclavicular joint arthritis, and glenohumeral arthritis. *Med Clin North Am* 2014; 98(4): 755-775.
2. Weishaupt D, Schweitzer ME. MR imaging of septic arthritis and rheumatoid arthritis of the shoulder. *Magn Reson Imaging Clin N Am* 2004; 12(1): 111-124.
3. Seifarth A, Roemer F. Systematik der glenohumeralen und akromioklavikulären Arthrose. *Radiologe* 2015; 55: 231-240.
4. Llauger J, Palmer J, Rosón N, et al. Nonseptic monoarthritis: imaging features with clinical and histopathologic correlation. *Radiographics* 2000; 20: S263-S278.
5. Sankaye P, Ostlere S. Arthritis at the shoulder joint. *Semin Musculoskelet Radiol* 2015; 19(3): 307-318.
6. Sussmann AR, Cohen J, Nomikos GC, et al. Magnetic resonance imaging of shoulder arthropathies. *Magn Reson Imaging Clin N Am* 2012; 20(2): 349-371.
7. Grainger AJ, McGonagle D. Imaging in rheumatology. *Imaging* 2003; 15(4): 286-297.
8. Lehtinen JT, Kaarela K, Belt EA, et al. Incidence of glenohumeral joint involvement in seropositive rheumatoid arthritis. A 15 year endpoint study. *J Rheumatol* 2000; 27(2): 347-350.
9. Petersson CJ. Painful shoulders in patients with rheumatoid arthritis. Prevalence, clinical and radiological features. *Scand J Rheumatol* 1986; 15(3): 275-279.
10. Thomas T, Noël E, Goupille P, et al. The rheumatoid shoulder: current consensus on diagnosis and treatment. *Joint Bone Spine* 2006; 73(2): 139-143.
11. Chen AL, Joseph TN, Zuckerman JD. Rheumatoid arthritis of the shoulder. *J Am Acad Orthop Surg* 2003; 11(1): 12-24.
12. Alasaarela E, Suramo I, Tervonen O, et al. Evaluation of humeral head erosions in RA: a comparison of ultrasonography, magnetic resonance imaging, computed tomography and plain radiography. *Br J Rheumatol* 1998; 37(11): 1152-1156.
13. Hermann KG, Backhaus M, Schneider U, et al. Rheumatoid arthritis of the shoulder joint: comparison of conventional radiography, ultrasound, and dynamic contrast-enhanced magnetic resonance imaging. *Arthritis Rheum* 2003; 48(12): 3338-3349.
14. Boesen M, Roemer FW, Østergaard M, et al. Imaging of common rheumatic joint diseases affecting the upper limb. *Radiol Clin North Am* 2019; 57(5): 1001-1034.
15. Amin MF, Ismail FM, El Shereef RR. The role of ultrasonography in early detection and monitoring of shoulder erosions, and disease activity in rheumatoid arthritis patients; comparison with MRI examination. *Acad Radiol* 2012; 19(6): 693-700.
16. Bruyn GA, Pineda C, Hernandez-Diaz C, et al. Validity of ultrasonography and measures of adult shoulder function and reliability of ultrasonography in detecting shoulder synovitis in patients with rheumatoid arthritis using magnetic resonance imaging as a gold standard. *Arthritis Care Res (Hoboken)* 2010; 62(8): 1079-1086.
17. Wakefield RJ, Balint PV, Szkudlarek M, et al. Musculoskeletal ultrasound including definitions for ultrasonic pathology. *J Rheumatol* 2005; 32: 2485-2487.
18. McQueen FM. The use of MRI in early RA. *Rheumatology (Oxford)* 2008; 47: 1597-1599.
19. Hetland ML, Ejbjerg B, Hørslev-Petersen K, et al. CIMESTRA study group. MRI bone oedema is the strongest predictor of subsequent radiographic progression in early rheumatoid arthritis: results from a 2-year randomised controlled trial (CIMESTRA). *Ann Rheum Dis* 2009; 68: 384-390.
20. Soker G, Bozkirli ED, Soker E, et al. Magnetic resonance imaging evaluation of shoulder joint in patients with early stage of ankylosing spondylitis: a case-control study. *Diagn Interv Imaging* 2016; 97(4): 419-424.
21. Falsetti P, Frediani B, Filippou G, et al. Enthesitis of proximal insertion of the deltoid in the course of seronegative spondyloarthritis. An atypical enthesitis that can mime impingement syndrome. *Scand J Rheumatol* 2002; 31(3): 158-162.
22. Davidson J. Juvenile idiopathic arthritis: a clinical overview. *Eur J Radiol* 2000; 33(2): 128-134.
23. Dabrowski W, Fonseka N, Ansell BM, et al. Shoulder problems in juvenile chronic polyarthritis. *Scand J Rheumatol* 1979; 8(1): 49-53.
24. Johnson K. Imaging of juvenile idiopathic arthritis. *Pediatr Radiol* 2006; 36(8): 743-758.
25. Chauvin NA, Jaimes C, Laor T, et al. Magnetic resonance imaging of the pediatric shoulder. *Magn Reson Imaging Clin N Am* 2012; 20(2): 327-347.

26. Leslie BM, Harris JM III, Driscoll D. Septic arthritis of the shoulder in adults. *J Bone Joint Surg Am* 1989; 71(10): 1516-1522.
27. O' Donnell PG, Ostlere SJ. Monoarthropathy. *Imaging* 1999; 11(2): 60-72.
28. Karchevsky M, Schweitzer ME, Morrison WB, et al. MRI findings of septic arthritis and associated osteomyelitis in adults. *AJR Am J Roentgenol* 2004; 182(1): 119-122.
29. Abdou MA, Jo A, Choi IS, et al. Shoulder joint infections with negative culture results: Clinical characteristics and treatment outcomes. *Biomed Res Int* 2019; 3756939.
30. Garcia-De La Torre I. Advances in the management of septic arthritis. *Infect Dis Clin North Am* 2006; 20(4):773-788.
31. Bierry G, Huang AJ, Chang CY, et al. MRI findings of treated bacterial septic arthritis. *Skeletal Radiol* 2012; 41: 1509-1516.
32. Davies AM, Hughes DE, Grimer RJ. Intramedullary and extramedullary fat globules on magnetic resonance imaging as a diagnostic sign for osteomyelitis. *Eur Radiol* 2005; 15: 2194-2199.
33. Bosworth BM. Calcium deposits in the shoulder and subacromial bursitis: a survey of 12,122 shoulders. *JAMA* 1941;116: 2477-2482.
34. Uhthoff HK, Loehr JW. Calcific tendinopathy of the rotator cuff: pathogenesis, diagnosis, and management. *J Am Acad Orthop Surg* 1997; 5(4): 183-191.
35. Farid N, Bruce D, Chung CB. Miscellaneous conditions of the shoulder: anatomical, clinical, and pictorial review emphasizing potential pitfalls in imaging diagnosis. *Eur J Radiol* 2008; 68(1): 88-105.
36. Depalma AF, Kruper JS. Long-term study of shoulder joints afflicted with and treated for calcific tendinitis. *Clin Orthop* 1961; 20: 61-72.
37. Chung CB, Gentili A, Chew FS. Calcific tendinitis and periarthritis: classic magnetic resonance imaging appearance and associated findings. *J Comput Assist Tomogr* 2004; 28(3): 390-396.
38. Flemming DJ, Murphey MD, Shekitka KM, et al. Osseous involvement in calcific tendinitis: a retrospective review of 50 cases. *AJR Am J Roentgenol* 2003; 181(4): 965-972.
39. Klontzas ME, Vassalou EE, Karantanas AH. Calcific tendinopathy of the shoulder with intraosseous extension: outcomes of ultrasound-guided percutaneous irrigation. *Skeletal Radiol* 2017; 46(2): 201-208.
40. Merolla G, Bhat MG, Paladini P, et al. Complications of calcific tendinitis of the shoulder: a concise review. *J Orthop Traumatol* 2015; 16: 175-183.
41. Baker CL Jr. Calcific tendinitis of the shoulder. *Orthop Clin North Am* 2003; 34(4): 567-575.
42. Gärtner J, Heyer A. Calcific tendinitis of the shoulder. *Orthopade* 1995; 24(3): 284-302.
43. Louwerens JK, Sierevelt IN, van Hove RP, et al. Prevalence of calcific deposits within the rotator cuff tendons in adults with and without subacromial pain syndrome: clinical and radiologic analysis of 1219 patients. *J Shoulder Elbow Surg* 2015; 24: 1588-1593.
44. Chianca V, Albano D, Messina C, et al. Rotator cuff calcific tendinopathy: from diagnosis to treatment. *Acta Biomed* 2018; 89(1-S): 186-196.
45. Bianchi S, Martinoli C. Ultrasound of the musculoskeletal system. Springer Berlin 2007, pp 189-331.
46. Chiou HJ, Chou YH, Wu JJ, et al. Evaluation of calcific tendonitis of the rotator cuff: role of color Doppler ultrasonography. *J Ultrasound Med* 2002; 21(3): 289-295.
47. Filippou G, Adinolfi A, Cimmino MA, et al. Diagnostic accuracy of ultrasound, conventional radiography and synovial fluid analysis in the diagnosis of calcium pyrophosphate dihydrate crystal deposition disease. *Clin Exp Rheumatol* 2016; 34(2): 254-260.
48. Loew M, Sabo D, Wehrle M, et al. Relationship between calcifying tendinitis and subacromial impingement: a prospective radiography and magnetic resonance imaging study. *J Shoulder Elbow Surg* 1996; 5(4): 314-319.
49. Mandrillo D, Psaras K, Karantanas A. Painful shoulder. *Hell J Radiol* 2016; 1(1): 78-81.
50. McCarty DJ. Milwaukee shoulder syndrome. *Trans Am Clin Climatol Assoc* 1991; 102: 271-283.
51. Jacques T, Michelin P, Badr S, et al. Conventional radiology in crystal arthritis. Gout, calcium pyrophosphate deposition and basic calcium phosphate crystals. *Radiol Clin North Am* 2017; 55(5): 967-984.
52. Omoumi P, Zufferey P, Malghem J, et al. Imaging in gout and other crystal-related arthropathies. *Rheum Dis Clin North Am* 2016; 42(4): 621-644.
53. Wong WD, Shah S, Murray N, et al. Advanced musculoskeletal applications of dual-energy computed tomography. *Radiol Clin North Am* 2018; 56(4): 587-600.
54. Neogi T, Jansen TL, Dalbeth N, et al. 2015 gout classification criteria: an American College of Rheumatology/ European League Against Rheumatism collaborative initiative. *Ann Rheum Dis* 2015; 74(10): 1789-1798.

55. Filippucci E, Delle Sedie A, Riente L, et al. Ultrasound imaging for the rheumatologist XLVII. Ultrasound of the shoulder in patients with gout and calcium pyrophosphate deposition disease. *Clin Exp Rheumatol* 2013; 31(5): 659-664.
56. Ottaviani S, Richette P, Allard A, et al. Ultrasonography in gout: a case-control study. *Clin Exp Rheumatol* 2012; 30(4): 499-504.
57. Richette P, Bardin T, Doherty M. An update on the epidemiology of calcium pyrophosphate dihydrate crystal deposition disease. *Rheumatology (Oxford)* 2009; 48(7): 711-715.
58. Gerster JC, Baud CA, Lagier R, et al. Tendon calcifications in chondrocalcinosis. A clinical, radiologic, histologic, and crystallographic study. *Arthritis Rheum* 1977; 20(2): 717-722.
59. Resnick D, Williams G, Weisman MH, et al. Rheumatoid arthritis and pseudo-rheumatoid arthritis in calcium pyrophosphate dihydrate crystal deposition disease. *Radiology* 1981; 140(3): 615-621.
60. Atalar AC, Sungur M, Demirhan M, et al. Neuropathic arthropathy of the shoulder associated with syringomyelia: a report of six cases. *Acta Orthop Traumatol Turc* 2010; 44(4): 328-336.
61. Rickert MM, Cannon JG, Kirkpatrick JS. Neuropathic arthropathy of the shoulder: A systematic review of classifications and treatments. *JBJS Rev* 2019; 7(10): e1. doi: 10.2106/JBJS.RVW.18.00155.
62. Laidlaw MS, Mahon HS, Werner BC. Etiology of shoulder arthritis in young patients. *Clin Sports Med* 2018; 37(4): 505-515.
63. Walsch G, Boulahia A, Boileau P, et al. Primary glenohumeral osteoarthritis: clinical and radiographic classification. The Aequalis group. *Acta Orthop Belg* 1998; 64 Suppl 2: 46-52.
64. Bock GW, Garcia A, Weisman MH, et al. Rapidly destructive hip disease: clinical and imaging abnormalities. *Radiology* 1993; 186: 461-466.
65. Ketapure AL, Sun JH, Sim GB, et al. Rapidly destructive arthrosis of the shoulder joints: radiographic, magnetic resonance imaging, and histopathologic findings. *J Shoulder Elbow Surg* 2015; 24: 922-927.
66. Flemming DF, Gustas-French CN. Rapidly progressive osteoarthritis: a review of the clinical and radiologic presentation. *Curr Rheumatol Rep* 2017; 19: 42.
67. Nguyen VD. Rapid destructive arthritis of the shoulder. *Skelet Radiol* 1996; 25: 107-112.
68. Eajazi A, Kussman S, LeBedis C, et al. Rotator cuff tear arthropathy: pathophysiology, imaging characteristics, and treatment options. *AJR Am J Roentgenol* 2015; 205(5): W502-W511.
69. Cofield RH, Parvizi J, Hoffmeyer PJ, et al. Surgical repair of chronic rotator cuff tears: a prospective long-term study. *J Bone Joint Surg Am* 2001; 83: 71-77.
70. Zumstein MA, Jost B, Hempel J, et al. The clinical and structural long-term results of open repair of massive tears of the rotator cuff. *J Bone Joint Surg Am* 2008; 90: 2423-2431.
71. Ecklund KJ, Lee TQ, Tibone J, et al. Rotator cuff tear arthropathy. *J Am Acad Orthop Surg* 2007; 15: 340-349.
72. Hamada K, Fukuda H, Mikasa M, et al. Roentgenographic findings in massive rotator cuff tears: a long-term observation. *Clin Orthop Relat Res* 1990; 254: 92-96.
73. Rokito AS, Cuomo F, Gallagher MA, et al. Long-term functional outcome of repair of large and massive chronic tears of the rotator cuff. *J Bone Joint Surg Am* 1999; 81: 991-997.
74. Zuckerman JD, Matsen FA III. Complications about the glenohumeral joint related to the use of screws and staples. *J Bone Joint Surg Am* 1984; 66(2): 175-180.
75. Alpay N, Artum-Esen B, Kamali S, et al. Amyloid arthropathy mimicking seronegative rheumatoid arthritis in multiple myeloma: case reports and review of the literature. *Amyloid* 2009; 16(4): 226-231.
76. Hughes TH, Sartoris DJ, Schweitzer ME, et al. Pigmented villonodular synovitis: MRI characteristics. *Skeletal Radiol* 1995; 24(1): 7-12.
77. Wahab H, Hasan O, Habib A, et al. Arthroscopic removal of loose bodies in synovial chondromatosis of shoulder joint, unusual location of rare disease: a case report and literature review. *Ann Med Surg (Lond)* 2018; 37: 25-29.

